Title
Tools for Operations Planning (TOPL1)

Author
Varaiya, Pravin

Publication Date
2008-06-01

CALIFORNIA PATH PROGRAM
INSTITUTE OF TRANSPORTATION STUDIES
UNIVERSITY OF CALIFORNIA, BERKELEY

Tools for Operations Planning (TOPL1)

Pravin Varaiya
University of California, Berkeley

California PATH Working Paper
UCB-ITS-PWP-2008-4

This work was performed as part of the California PATH Program of the University of California, in cooperation with the State of California Business, Transportation, and Housing Agency, Department of Transportation, and the United States Department Transportation, Federal Highway Administration.

Final Report for Task Order 6611

June 2008

ISSN 1055-1417

Tools for Operations Planning (TOPL1)
Final Report for PATH TO 6611
Pravin Varaiya

Department of Electrical Engineering and Computer Science

University of California, Berkeley CA 94720

Tel: (510) 642-5270, Fax: (510) 642-7815

varaiya@eecs.berkeley.edu

April 17, 2008

Abstract

TOPL is a suite of tools to (1) specify operational improvements including ramp metering, incident and demand management, auxiliary lanes, traveler information and (2) quickly estimate the benefits that such improvements can realize. TOPL is based on the macroscopic cell transmission model (CTM). Version 1, TOPL1, provides preliminary software packages, a calibrated model of 880N.

The website of the TOPL project is http://path.berkeley.edu/topl/

Keywords: Corridor management, macroscopic simulation, cell transmission model, model calibration

A full color version of this paper is available on-line at http://www.path.berkeley.edu in the publications section

2. Summary of accomplishments

TOPL1 developed preliminary versions of three software packages: FM (Freeway Modeler), CTMSim and Aurora1. All are based on the same macroscopic cell transmission model (CTM), so they are consistent with each other. FM and CTMSim model a single freeway. Aurora models a freeway corridor, i.e., a road *network* with freeways and arterials. Thus Aurora is much more general. The packages also come with several ramp controllers that the user can employ to evaluate their impact.

2.1 CTM Theory

We summarize the results of our theoretical investigation of the CTM model. The full discussion (Gomes et al, 2007) is appended.

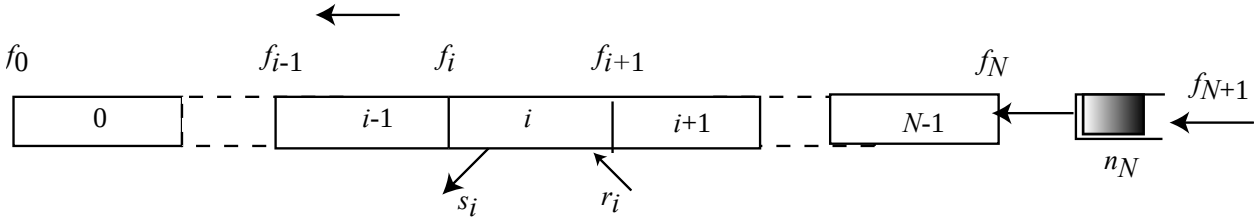

Figure 1 Freeway model

Fig. 1 shows the freeway divided into N sections, each with one on- and one off-ramp. Vehicles move from right to left. Section i is upstream of section i-1. There are two boundary conditions. Free flow prevails downstream of section 0; upstream of the freeway is an ‘‘on-ramp’’ with an inflow of r_N. The flow accepted by section N-1 is $f_N(k)$ vehicles per period or time step k. On-ramp flows are given as demand. Off-ramp flows are determined by specified split ratios.

The state of the system is given by the N-dimensional vector n of vehicle densities in the N sections. Intra-cell changes in the state are determined by flow conservation. Inter-cell flows are determined by the fundamental diagram.

A feasible stationary demand pattern induces a unique equilibrium flow in each section. However, there is an infinite set—in fact a continuum—of equilibrium states, including a unique uncongested equilibrium n^u in which free flow speed prevails in all sections, and a unique most congested equilibrium n^{con}. In every other equilibrium ne one or more sections are congested, and $n^u \le n \le n^{con}$. Every equilibrium is stable and every trajectory converges to some equilibrium state.

Two implications for ramp metering are explored. First, if the demand exceeds capacity and the ramps are not metered, every trajectory converges to the most congested equilibrium. Moreover, there is a ramp metering strategy that increases discharge flows and reduces total travel time compared with the no-metering strategy. Second, even when the demand is feasible but the freeway is initially congested, there is a ramp metering strategy that moves the system to the uncongested equilibrium and reduces total travel time. The two conclusions show that congestion invariably indicates wastefulness of freeway resources that ramp metering can eliminate.

2.2 Simulation

We summarize results of the 880N simulation.

Figure 2 Map of 880N with major bottlenecks

Figure 2 is a map of 880N, a 45-mile long freeway in the San Francisco Bay Are stretching from San Jose in the South to Oakland in the North. The map shows the location of two major bottlenecks.

The bottlenecks are visible in the speed contour plots for four days shown in Figure 3. There are several other bottlenecks as well. Observe in on all four plots congestion starts at a bottleneck and moves upstream, forming the characteristic low speed triangles, as predicted by Theorem 4.1 of (Gomes et al, 2007).

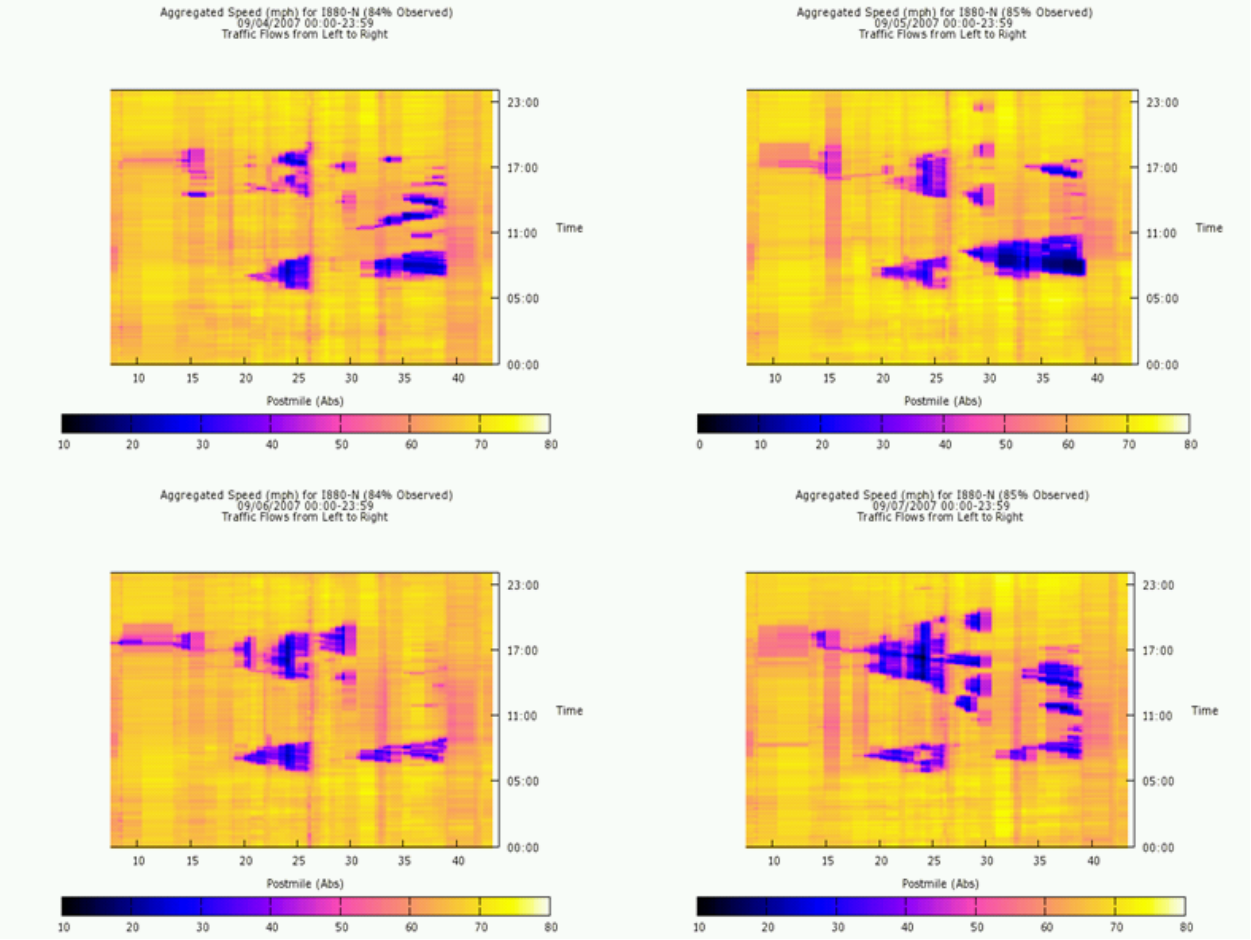

Figure 3 Speed contour plots for I-880N for four days, 4-7 September, 2007. Source: PeMS

Figure 4 is a screen shot of a display window of the TOPL simulation of I-880N for the base case. The window is divided into two halves. The right-hand side displays contour plots of flow (top), density (middle) and speed (bottom). The left-hand side displays five performance plots: (instantaneous) travel time, VMT, VHT, delay and productivity loss. Comparisons with empirical data indicate that the estimated CTM model conforms reasonably well with measurement. For example, the contour plots clearly show the two major bottlenecks. Similarly, the delay in the morning peak is much larger than the afternoon peak, which is to be expected, because the morning commute direction is north. These and other comparisons lend confidence to the results of the scenario analysis presented in (Varaiya, 2008). That paper is appended as well.

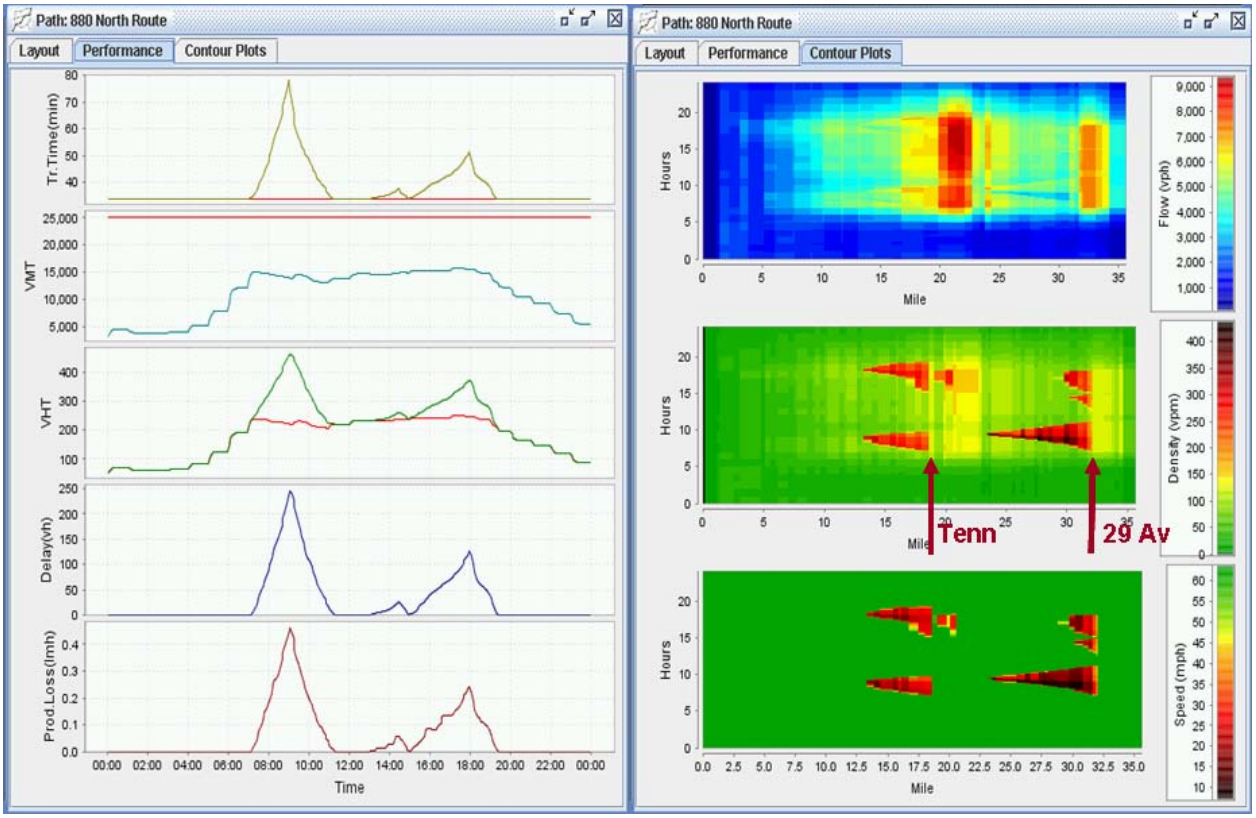

Figure 4 TOPL simulation of the 880N base case

3. Conclusion

In November, 2006 California voters approved a $20 billion bond measure to improve transportation. Subsequently, the California Department of Transportation (Caltrans) launched an ambitious "corridor management program (CMP)" to design and implement operational improvements---emphasizing ramp metering, incident management, traveler information, and demand management (including using tolls)---that would reduce congestion in 2025 by 40 percent (California Department of Transportation, 2006).

TOPL is our response to the needs of the CMP by developing a set for (1) specifying such operational improvements and (2) quickly estimating the benefits such improvements are likely to provide. At the end of the first year of effort, the TOPL approach appears very likely to meet its goals.

Acknowledgement

TOPL is supported by the California Department of Transportation through the California PATH Program. The contents of this paper reflect the views of the author and not necessarily the official views or policy of the California Department of Transportation. The results reported here are due to the TOPL Group, especially Gabriel Gomes, Roberto Horowitz, Alex Kurzhanskiy and Jaimyoung Kwon. It is a pleasure to acknowledge the criticisms and encouragement of John Wolf, Pat Weston and Carlos Ruiz of Caltrans; Alex Skabardonis of PATH; Tarek Hatata of System Metrics Group; and Vassili Alexiadis of Cambridge Systematics.

References

California Department of Transportation. Strategic Growth Plan, 2006 www.dot.ca.gov/docs/strategicgrowth.pdf-2006-10-10.

G. Gomes et al (2007). Behavior of the Cell Transmission Model and Effectiveness of Ramp Metering.*Transportation Research, Part C,* (in press), available online www.sciencedirect.com

P. Varaya (2008). TOPL: Tools for Operations Planning. To be presented at 10th International Conference on Applications of Advanced Technologies in Transportation (AATT 2008), Athens, Greece, May 28-30, 2008.

For more information please see: http://path.berkeley.edu/topl/papers/2007TRC__CTMBehavior.pdf

TOPL: TOOLS FOR OPERATIONS PLANNING

Pravin Varaiya[1]

ABSTRACT. TOPL is a suite of software tools for specifying freeway operational improvement strategies, such as ramp metering, demand and incident management, and for quickly estimating the benefits of such improvements. TOPL is based on the macroscopic cell transmission model. The paper summarizes the theory of the cell transmission model and describes the procedure to carry out a TOPL application. The procedure is illustrated for the 45-mile long I-880N freeway in California, whose model is calibrated using loop detector measurements of volume and speed. The measurements show that congestion originates in a bottleneck and moves upstream, as predicted by the theory. The simulations show that appropriate ramp metering can dramatically reduce total congestion delay and mainline travel time.

INTRODUCTION

In November, 2006 California voters approved a $20 billion bond measure to improve transportation. Subsequently, the California Department of Transportation (Caltrans) launched an ambitious 'corridor management program' to design and implement operational improvements—emphasizing ramp metering, incident management, traveler information, and demand management (including using tolls)—that would reduce congestion in 2025 by 40 percent (California Department of Transportation (2006)). This paper describes TOPL (Tools for Operations Planning), a suite of software tools for (1) specifying such operational improvements and (2) quickly estimating the benefits such improvements are likely to provide.

TOPL is based on the macroscopic cell transmission model (CTM). Traditionally, such investigations favor use of microscopic models, and indeed Caltrans has let contracts for microsimulation models. However, the required data collection and model calibration effort has significantly slowed this effort (California Center for Innovative Transportation (2006)). By contrast, the CTM model is based on aggregate variables such as volume

[1]Nortel Networks Distinguished Professor, Department of Electrical Engineering and Computer Sciences, University of California, Berkeley, CA 94720 USA, email: varaiya@eecs.berkeley.edu

or flow and density, which for California freeways, are routinely measured and archived (PeMS (2007)). Consequently, TOPL models are very quickly specified, calibrated and run to generate useful results.

CTM and its properties are reviewed in the next two sections, which are based on Gomes et al. (2007). The subsequent section briefly summarizes the steps within TOPL to describe and calibrate a CTM model. This is followed by a TOPL application for the 40-mile long I-880N freeway in the San Francisco Bay Area.

CELL TRANSMISSION MODEL

The notation used here and the properties of the model stated below as Propositions 1-3 are from (Gomes et al. (2007)). Figure 1 shows the freeway divided into N sections or cells, each with one on- and one off-ramp. Vehicles move from right to left. There are two boundary conditions. Free flow prevails downstream of section 0, and vehicles from upstream of the freeway enter an "on-ramp" with specified inflow r_N. The flow accepted by section $(N-1)$ is $f_N(k)$ vehicles in period k. The cumulative difference forms a queue of size $n_N(k)$.

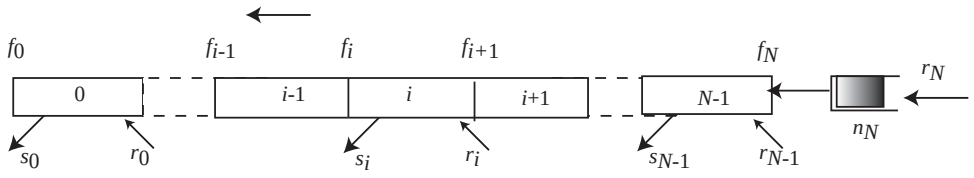

Figure 1: The freeway has N sections. Each section has one on- and one off-ramp.

Symbol	Name	Value	Unit
	section length	1	miles
	period	0.01	hours
F_i	capacity per lane	20	veh/period
v_i	free flow speed	0.6	section/period
w_i	congestion wave speed	0.2	section/period
n_i^c	critical density	33	veh/section
$\bar{n}_i$	jam density	133	veh/section
β_i	split ratio	$\in [0,1)$	dimensionless
$\bar{\beta}_i$	complementary split ratio $= 1-\beta_i$	$\in (0,1]$	dimensionless
k	period number	integer	dimensionless
$f_i(k)$	flow from section i to $i-1$ in period k	variable	veh/period
$s_i(k), r_i(k)$	off-ramp, on-ramp flow in section i in period k	variable	veh/period
$n_i(k)$	number of vehicles in section i in period k	variable	veh/section

Table 1: Model variables and parameters.

Table 1 lists the model variables and parameters with plausible values, e.g. , capacity 20 veh/period/lane or 2,000 vehicles/hour/lane, and free flow speed 0.6 sections/period or 60 mph. The length of all sections is normalized to 1 by absorbing differences in length in the speeds v_i, w_i. To be physically meaningful vehicles should not cross an entire cell

in one period, so $0 < v_i, w_i < 1$. The off-ramp flow is assumed to be a portion $\beta_i(k)$ of the total flow leaving the section:

$$s_i(k) = \beta_i(k)(s_i(k) + f_i(k)), \text{ or } s_i(k) = [\beta_i(k)/(1 - \beta_i(k))]f_i(k).$$

Assume constant split ratios β_i ($\beta_N = 0$). With $\bar{\beta}_i = 1 - \beta_i$, the model is, for $k \geq 0$,

$$\begin{aligned}
n_i(k+1) &= n_i(k) - f_i(k)/\bar{\beta}_i + f_{i+1}(k) + r_i(k), \quad 0 \leq i \leq N-1, && (1)\\
f_i(k) &= \min\{\bar{\beta}_i\, v_i\, n_i(k), w_{i-1}[\bar{n}_{i-1} - n_{i-1}(k)], F_i\}, \quad 1 \leq i \leq N, && (2)\\
f_0(k) &= \min\{\bar{\beta}_0\, v_0\, n_0(k), F_0\}, && (3)\\
n_N(k+1) &= n_N(k) - f_N(k) + r_N(k). && (4)
\end{aligned}$$

Flow conservation in section $i \leq N-1$ is expressed by

$$n_i(k+1) = n_i(k) - f_i(k) + f_{i+1}(k) + r_i(k) - s_i(k), \quad (5)$$

which is equivalent to (1), using $s_i(k) = \beta_i/\bar{\beta}_i f_i(k)$; and in section N by (4). The flow $f_i(k)$ from section i to $i-1$ is governed by the 'fundamental diagram' (2) with this interpretation: $\bar{\beta}_i v_i n_i(k)$ is the number of vehicles that can move from section i to $i-1$ in period k; $w_{i-1}[\bar{n}_{i-1} - n_{i-1}(k)]$ is the number that $i-1$ can accept; and F_i is the *capacity* or maximum possible flow from section i to $i-1$. Equation (3) indicates there is no congestion downstream of section 0. It is tacitly assumed that the flows $s_i(k)$ are not constrained by off-ramp capacity.

The parameter values in Table 1 correspond to the fundamental diagram of Figure 2. The

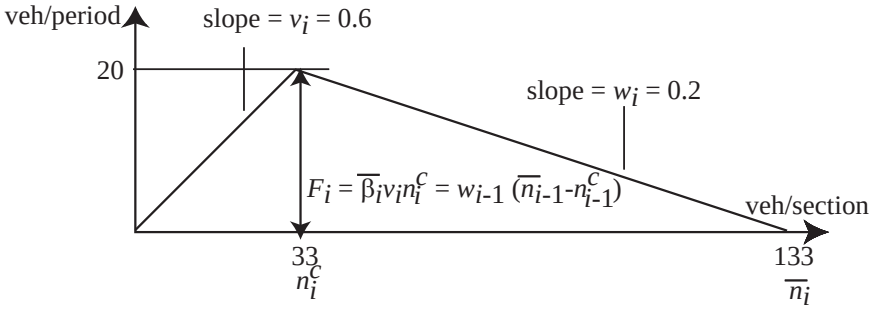

Figure 2: The fundamental diagram is characterized by capacity F_i and speeds v_i, w_i.

state of the system is the N-dimensional vector $n(k) = (n_0(k), \cdots, n_{N-1}(k))$.

Assume stationary demands $r_i(k) \equiv r_i$. Each on-ramp *demand* vector $r = (r_0, \cdots, r_N)$ induces a unique *equilibrium flow* vector $f(r) = (f_0, \cdots, f_N)$ calculated from

$$\begin{aligned}
f_N &= r_N, && (6)\\
f_i &= \bar{\beta}_i\,(f_{i+1} + r_i), \quad 0 \leq i \leq N-1. && (7)
\end{aligned}$$

Demand r is said to be *feasible* if $0 \leq f_i \leq F_i$, $0 \leq i \leq N$; *strictly feasible* if $0 \leq f_i < F_i$, $0 \leq i \leq N$; and *infeasible* if $f_i > F_i$ for some i.

$n = (n_0, \cdots, n_{N-1})$ is an *equilibrium state* for a feasible demand r if the trajectory $n(k) \equiv n$ is a solution of (1)-(3), i.e.,

$$f_i = \min\{\bar{\beta}_i\, v_i\, n_i, F_i - w_{i-1}[n_{i-1} - n^c_{i-1}], F_i\}, \quad 1 \le i \le N-1, \tag{8}$$
$$f_0 = \min\{\bar{\beta}_0\, v_0\, n_0, F_0\}. \tag{9}$$

At equilibrium n, section i is *uncongested* if $0 \le n_i \le n^c_i$ and *congested* if $n_i > n^c_i$; the equilibrium n is *uncongested* if all sections are uncongested; otherwise it is congested. In an uncongested section, free flow speed prevails; in a congested section, speed is lower.

Proposition 1 *A feasible demand r has a unique uncongested equilibrium $n^u(r)$:*

$$n^u_i(r) = (\bar{\beta}_i\, v_i)^{-1} f_i(r), \quad 0 \le i \le N-1. \tag{10}$$

In addition to the uncongested equilibrium (10), there is an *infinite* number—in fact, a continuum—of congested equilibria. Let $E = E(r)$ be the set of equilibria, i.e., the set of all solutions of the system of nonlinear equations (8)-(9).

Say that section i is a *bottleneck* for a feasible demand r (or equilibrium flow f) if $f_i = F_i$, i.e., in a bottleneck flow equals capacity. Suppose there are $K \ge 0$ bottlenecks at $0 \le I_1 < I_2 < \cdots < I_K \le N-1$. Partition the freeway into $1+K$ segments $S^0, \cdots, S^K$ comprising contiguous sections as follows:

$$S^0 = \{0, \cdots, I_1 - 1\},\ S^1 = \{I_1, \cdots, I_2 - 1\}, \cdots,\ S^K = \{I_K, \cdots, N-1\}. \tag{11}$$

If demand is strictly feasible, there is no bottleneck, so $K = 0$, $I_1 = N$ and segment $S^0 = \{0, \cdots, N-1\}$ is the entire freeway. On the other hand, if the most downstream section is congested, $I_1 = 0$ and S^0 is the empty segment.

Partition the state vector $n = (n_0, \cdots, n_{N-1})$ into sub-vectors $n = (n^0, \cdots, n^K)$ in conformity with segments $S^0, \cdots, S^K$, so n^k has components n_i, $i \in S^k$. The equilibrium conditions (8)-(9) partition into $1+K$ *decoupled* conditions, one for each segment. These decoupled conditions decompose the equilibrium set into a product,

$$E(r) = E^0(r) \times \cdots \times E^K(r). \tag{12}$$

Since S^0 is uncongested, $E^0(r)$ consists of the unique uncongested equilibrium $n^{u,0}(r)$ given by (see (10))

$$n^{u,0}_i(r) = (\bar{\beta}_i\, v_i)^{-1} f_i, \quad i \in S^0.$$

For $k \ge 1$, the terms $E^k(r)$ in (12) have a similar structure, differing only in the number of sections in S^k. To explore this structure, consider a generic segment $S = \{0, \cdots, N-1\}$ with N cells and a demand r with equilibrium flow $f = (f_0, \cdots, f_{N-1})$ with $f_0 = F_0$ and $f_i < F_i, i > 0$. Let E be the set of equilibria. Proposition 2 characterizes E.

In addition to the uncongested density $n^u_i(r)$ define the *congested* density

$$n^{con}_i(r) = n^c_i + w_i^{-1}(F_{i+1} - f_{i+1}). \tag{13}$$

Then

$$n_i^u(r) \le n_i^c \le n_i^{con}, \quad i = 0, \cdots, N-1.$$

Denote $\tilde{n}^{-1} = n^u$, the uncongested equilibrium (10), and

$$\tilde{n}^k = (n_0^{con}, \cdots, n_{k-1}^{con}, n_k^u, \cdots, n_{N-1}^u), \quad k = 0, \cdots N-1. \tag{14}$$

In state $\tilde{n}^k$ the first k sections are congested, the rest are uncongested.

Proposition 2 *The set of equilibria $E \subset R^N$ can be expressed geometrically as*

$$E = [\tilde{n}^{-1}, \tilde{n}^0] \cup [\tilde{n}^0, \tilde{n}^1] \cup \cdots \cup [\tilde{n}^{N-2}, \tilde{n}^{N-1}], \tag{15}$$

in which $[\tilde{n}^{k-1}, \tilde{n}^k]$ denotes the straight line segment joining $\tilde{n}^{k-1}$ and $\tilde{n}^k$.

Figure 3 illustrates Proposition 2 for a three-section freeway in which section 0 is the only bottleneck ($f_0 = F_0, f_1 < F_1, f_2 < F_2$). The flows determine the equilibrium set (15), which for this example comprises the three straight line segments shown in the bottom of the figure.

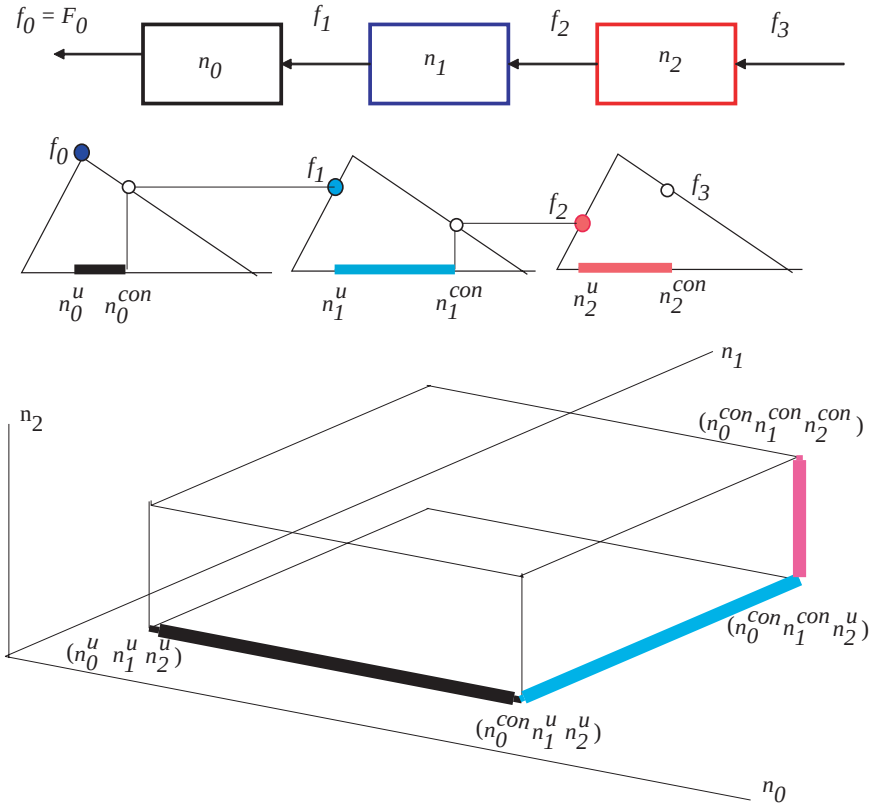

Figure 3: Illustration of Proposition 2 for a three-section segment.

Two important observations follow from Proposition 2. First, congestion starts at a bottleneck section and spreads upstream. Thus, in the freeway of Figure 3, the bottleneck

section 0 must be congested before section 1 can become congested, and section 1 must be congested before section 2 can become congested. Second, the flows in all sections are the *same* at every equilibrium in the set (15), even though at (say) the equilibrium n^u no section is congested and vehicles move at free flow speed, whereas at $\tilde{n}^{N-1}$ every section is congested and vehicles move at lower speed. Thus the presence of congestion is *not* an indication of excess demand.

EXCESSIVE DEMAND AND EFFICIENT RAMP METERING

In peak hours demand may be infeasible, and the preceding analysis needs modification.

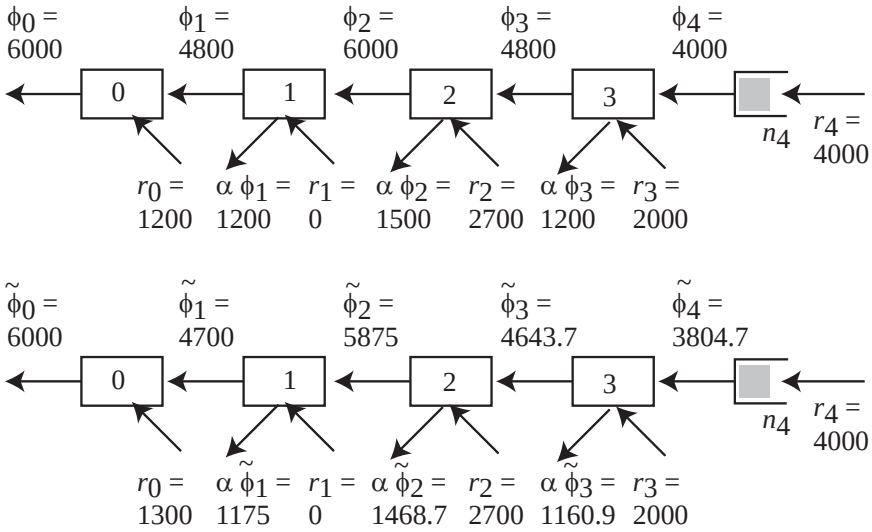

Figure 4: Freeway, on-ramp and off-ramp flows of Example 2: feasible demand (top); excessive demand (bottom).

Example The upper part of Figure 4 displays a freeway with four identical three-lane sections, each lane characterized by the fundamental diagram in Figure 2, so each section has capacity of 6000 vph. The demand $r = (r_0 = 1200, r_1 = 0, r_2 = 2700, r_3 = 2000, r_4 = 4000)$. $\beta_0 = 0$; all other split ratios are the same: $\beta_i = \beta = 0.2$, so $\bar{\beta} = 0.8$. Denote $\alpha = \beta[\bar{\beta}]^{-1} = 0.25$. The demand r is feasible and the equilibrium flow $\phi = (\phi_0 = 6000, \phi_1 = 4800, \phi_2 = 6000, \phi_3 = 4800, \phi_4 = 4000)$. The off-ramp flow in section i is $\alpha\phi_i$. Sections 0 and 2 are bottlenecks, with equilibrium flows equal to capacity.

Suppose demand increases to $\tilde{r}$, with $\tilde{r}_0 = 1300 > r_1$ and $\tilde{r}_i = r_i, i \geq 0$. This demand is *infeasible* because it would increase ϕ_0 to $\phi_1 + \tilde{r}_0 = 6100$, which exceeds capacity. The increased on-ramp flow in section 0 will create congestion in section 0 and force a reduction in the flow out of section 1 from $\phi_1 = 4800$ to $\tilde{\phi}_1 = 4700$. This reduction propagates upstream and ultimately reduces the flow out of section 4 from $\phi_4 = 4000$ to $\tilde{\phi}_4 = 3804.6875$. The on-ramp queue n_4 will grow at the rate of $4000 - 3804.6875 = 195.3125$ vph. All sections will become congested. The discharge at the off-ramps will be reduced from $\alpha\phi_i$ to $\alpha\tilde{\phi}_i$. The new equilibrium flows are displayed in the lower part Figure 4.

Thus the infeasible demand $\tilde{r}$ leads to a unique equilibrium flow $\tilde{\phi}$, corresponding to the lower, *feasible* demand $\tilde{r}^f$, which is the same as $\tilde{r}$, except that the upstream flow is reduced from $\phi_4 = 4000$ to $\tilde{\phi}_4 \approx 3804$. The system converges to the most congested equilibrium corresponding to $\tilde{r}^f$.

For demand $r = (r_0, \cdots, r_N)$, let ϕ be the solution of (6)-(7):

$$\phi_N = r_N, \quad \phi_i = \bar{\beta}_i(\phi_{i+1} + r_i), \quad 0 \le i \le N-1.$$

Suppose that r is *infeasible*, so that $\phi_i > F_i$ for some i. To simplify the notation assume that $\phi_0 > F_0$. Assume that the demand becomes feasible if either $r_N = 0$ or $r_0 = 0$. Let

$$\tilde{r}_N = \max\{\rho \ge 0 \mid \text{ the demand } (r_0, \cdots, r_{N-1}, \rho) \text{ is feasible}\} \tag{16}$$

$$\hat{r}_0 = \max\{\rho \ge 0 \mid \text{ the demand } (\rho, r_1, \cdots, r_N) \text{ is feasible}\} \tag{17}$$

Proposition 3 *(i) $\tilde{r}_N < r_N$ is the largest upstream flow for which the demand $\tilde{r} = (r_0, \cdots, r_{N-1}, \tilde{r}_N)$ is feasible. The corresponding equilibrium flow $\tilde{\phi}$ is*

$$\tilde{\phi}_N = \tilde{r}_N, \quad \phi_i = \bar{\beta}_i(\tilde{\phi}_{i+1} + r_i), \quad 0 \le i \le N-1.$$

(ii) With demand r, under the no-metering strategy the system converges to the (unique) most congested equilibrium $n^{con} \in E(\tilde{r})$ corresponding to demand $\tilde{r}$. The queue $n_N(k)$ at the upstream ramp grows at the rate of $(r_N - \tilde{r}_N)$ vehicles per period.
(iii) $\hat{r}_0 < r_0$ is the largest flow for which the demand $\hat{r} = (\hat{r}_0, r_1, \cdots, r_N)$ is feasible. The corresponding equilibrium flow $\hat{\phi}$ is

$$\hat{\phi}_N = r_N, \ \hat{\phi}_i = \bar{\beta}_i(\hat{\phi}_{i+1} + r_i), \ 1 \le i \le N-1, \ \hat{\phi}_0 = \bar{\beta}_0(\hat{\phi}_1 + \hat{r}_0).$$

Under the ramp metering strategy that reduces the on-ramp flow in section 0 from r_0 to $\hat{r}_0$, the system converges to some equilibrium in $E(\hat{r})$. The queue at the on-ramp in section 0 grows at the rate of $(r_0 - \hat{r}_0)$ vehicles per period.
(iv) Flows under the ramp-metering strategy are larger throughout the freeway:

$$\tilde{\phi}_i < \hat{\phi}_i, \ 1 \le i \le N \text{ and } \tilde{\phi}_0 = \hat{\phi}_0 = F_0.$$

Suppose $\beta_i > 0$ for some $i \ge 1$, so that there is non-zero off-ramp flow in at least one section. Then the total discharge under the ramp-metering strategy is strictly larger than under the no-metering strategy. Moreover,

$$\mu = \frac{r_N - \tilde{r}_N}{r_0 - \hat{r}_0} = (\bar{\beta}_1 \cdots \bar{\beta}_N)^{-1} > 1. \tag{18}$$

Substituting the split ratios of Example 2 into (18) gives the ramp metering 'gain'

$$\mu = (\bar{\beta}_1 \bar{\beta}_2 \bar{\beta}_3) = (0.8)^{-3} \approx 2.$$

The next result is not difficult to prove.

Proposition 4 *There is a ramp metering strategy that achieves the metering gain (18). With a small sacrifice in capacity, the strategy achieves the uncongested equilibrium.*

TOPL PROCEDURE

Simulation of a freeway requires five steps:

Step 1 Network specification. The freeway network must be defined in the form of Figure 1, i.e., the freeway must be divided into cells, each with (at most) one on- and one off-ramp. Each cell should be homogeneous in terms of number of lanes and grade, so that it is sensible to represent the behavior of traffic in the cell by a single fundamental diagram. In order to facilitate calibration, as far as possible, each cell should have a vehicle detector station that measures volume and speed.

In TOPL, network specification begins with a GIS map from which the freeway geometry (number of lanes and position of ramps) is extracted. An algorithm takes the specified geometry and the location of detector stations, obtained from (PeMS (2007)) and produces a cell division of the freeway. The resulting cell structure is manually inspected and changed if needed.

Step 2 Fundamental diagram. Five-minute average measurements of volume and speed over several days are collected from each functioning detector. A triangular fundamental diagram in the form of Figure 2 is fitted to the data. This leads to the specification of each cell that has a detector. For those cells that do not have a detector a 'default' fundamental diagram is specified. (In practice average values of the parameters of estimated fundamental diagrams are taken as default values.)

Step 3 Ramp flows. Data for on- and off-ramp flows are collected. All too often, these data are missing or incorrect. TOPL has an elaborate procedure to impute missing and incorrect ramp data. The basic idea is as follows. Suppose the on-ramp flow sequence, $r_i(k)$, is missing. The procedure assumes a certain profile $\hat{r}_i(k)$, calculates the resulting density profile $\hat{n}_i(k)$ (using the fundamental diagram obtained in Step 2), compares this density with the measured density profile $n_i(k)$, and changes the assumed profile $\hat{r}_i(k)$ so as to reduce the 'error' $\sum |n_i(k) - \hat{n}_i(k)|$. This procedure is repeated until the error is acceptable. The ramp flows are now used to generate split ratios, which are usually time-varying.

Step 4 Base case. At the end of Steps 1-3, the CTM model is fully specified. The model is run for a 'base case', which simply means a particular day or several days for which good data are available. The model output is compared with actual field data in terms of (1) location of bottlenecks and speed contour plots, (2) hourly delays, (3) travel time, and other performance measures.

Step 5 Scenarios. Several scenarios are specified. A scenario is created by specifying changes in the fundamental diagram and in the on-ramp demand. These inc;lude (1) increasing demand by (say) two percent relative to the base case; (2) modeling an incident in a particular cell by reducing the capacity of the cell by one or two lanes for a certain time period; (3) a demand management scheme that reduces on-ramp flows at some locations by

a certain amount. TOPL provides several ramp metering control laws, including ALINEA (Papageorgiou et al. (1991, 1997)) and those described in (Sun and Horowitz (2006)). Running each specified scenario with and without ramp metering in place provides an estimate of the benefits of ramp metering.

TOPL APPLICATION: I-880N

This section is devoted to a TOPL case study of I-880N, a 45-mile long freeway in the San Francisco Bay Are stretching from San Jose in the South to Oakland in the North, shown in the map of Figure 5. The map shows the location of two major bottlenecks. The bottlenecks are visible in the speed contour plots for four days shown in Figure 6.

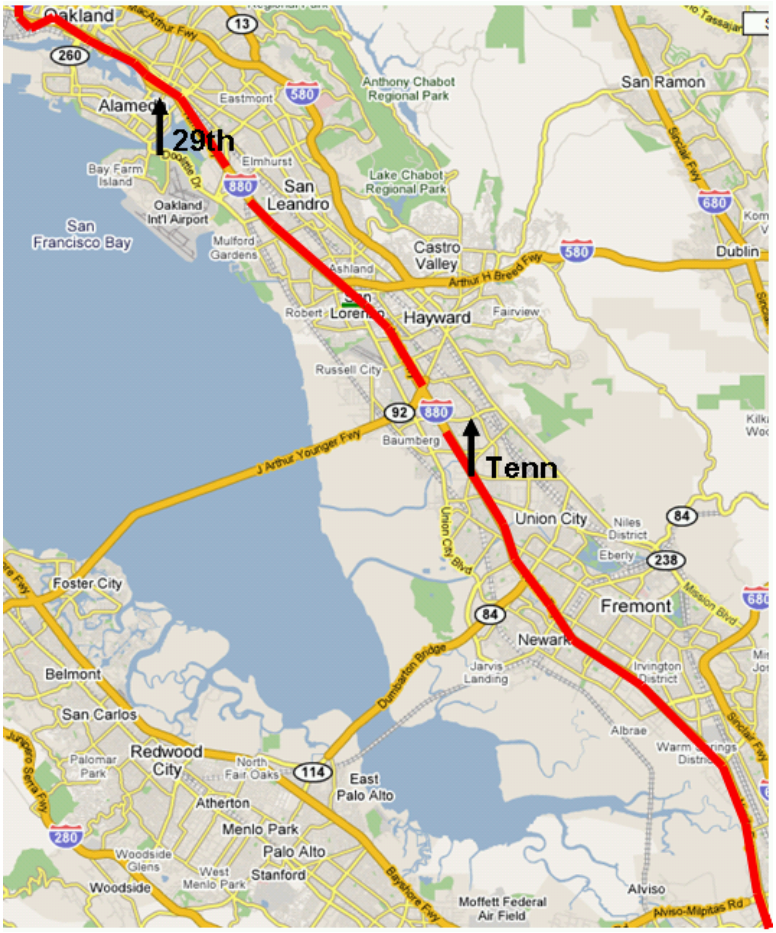

Figure 5: I-880N with location of two major bottlenecks at 29th and Tennyson Avenues.

There are several other bottlenecks as well. Observe in on all four plots congestion starts at a bottleneck and moves upstream, forming the characteristic low speed triangles, as predicted by Proposition 2.

Figure 7 is a screen shot of a display window of the TOPL simulation of I-880N for the base case. The window is divided into two halves. The right-hand side displays contour plots of flow (top), density (middle) and speed (bottom). The left-hand side displays five performance plots: (instantaneous) travel time, VMT, VHT, delay and productivity loss. Comparisons with empirical data indicate that the estimated CTM model conforms

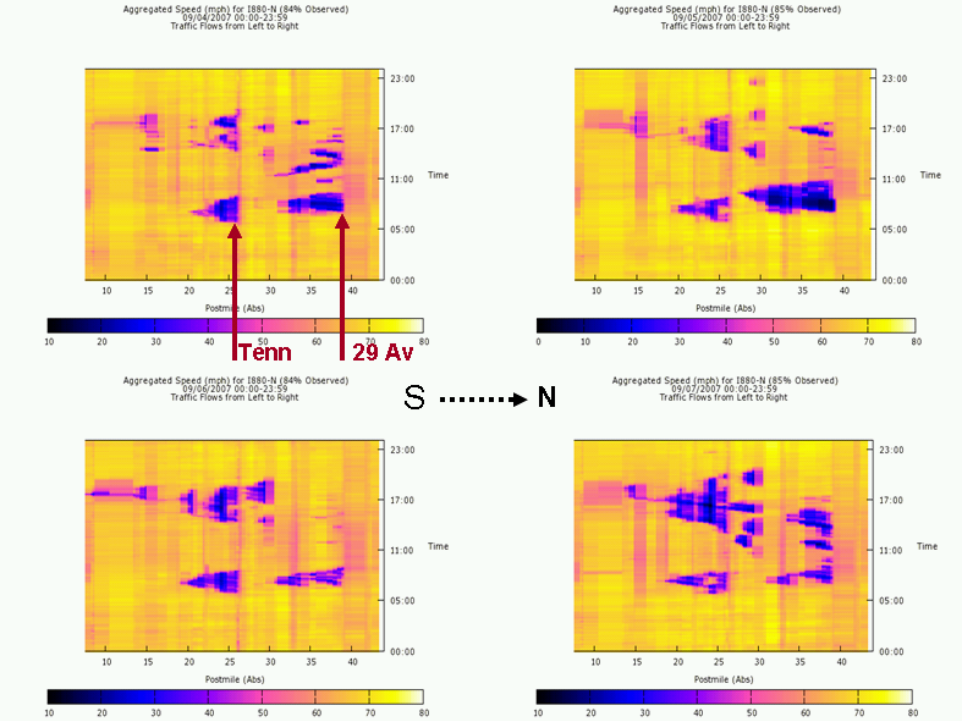

Figure 6: Speed contour plots for I-880N for four days, 4-7 September, 2007: Source PeMS (2007).

reasonably well with measurement. For example, the contour plots clearly show the two major bottlenecks. Similarly, the delay in the morning peak is much larger than the afternoon peak, which is to be expected, because the morning commute direction is north. These and other comparisons lend confidence to the results of the scenario analysis considered next.

On 27 September, 2007, there was a serious accident at 3:40PM. The accident is simulated as a reduction in the capacity (two of four lanes were shut down) from 3:40PM until 4:45PM. Figure 8 shows the results of the simulation, with the density contour replaced by the measured speed contour. The location and time of occurrence of the accident is indicated by **X**. The two ellipses mark the increase delay and congestion caused by the accident, in comparison with the base case of Figure 7. The reduction in capacity causes the demand to be infeasible, and congestion spreads as predicted by Proposition 3.

Figure 9 shows the reduction in the congestion impact of the accident by ramp metering. The freeway is maintained in free flow, as suggested by Proposition 4. The dotted ellipses are in the same locations as the solid ellipses of Figure 8. Of course, free flow on the mainline is partly paid for by delay on the ramps. Nonetheless, there is a net reduction in delay as summarized in Figure 10. The figure plots hourly delay (including delay on the ramps) for three scenarios: base case (blue), accident with no metering (red), and accident with metering (green). The area between the red and green plots is the net delay savings due to ramp metering.

A more dramatic scenario is illustrated in Figures 11 which simulates the impact of a two percent increase in demand (all on-ramp flows are increased by two percent relative to

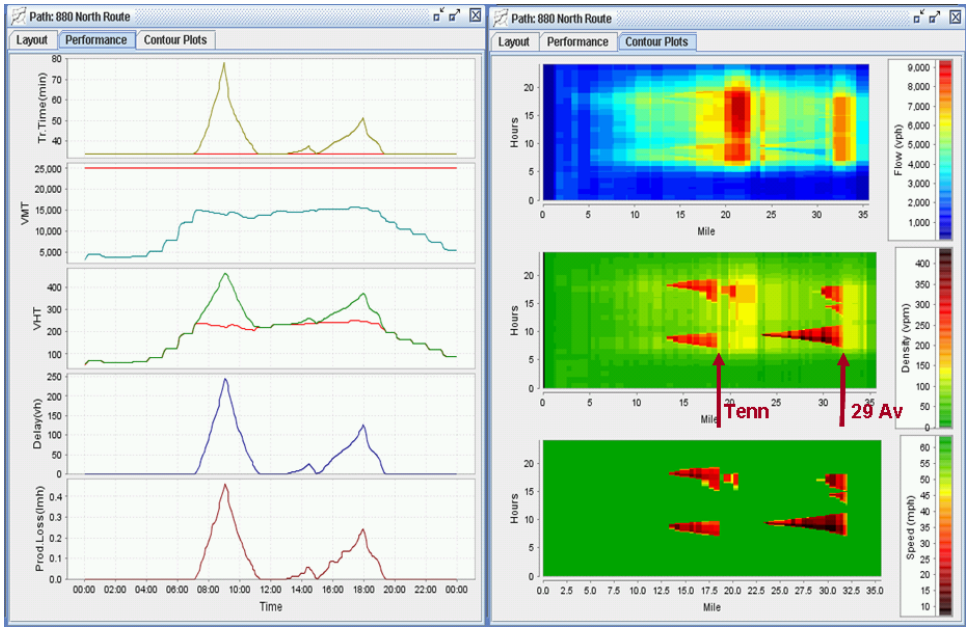

Figure 7: I-880 simulation of the base case.

the base case). The morning congestion does not disappear by mid-day as in the base case of Figure 7, and as a result congestion in the afternoon peak is worse. Nevertheless, ramp metering keeps the mainline free flowing as indicated in Figure 12. The net effect is summarized in the hourly delay plots of Figure 13, which is analogous to Figure 10.

CONCLUSIONS

The macroscopic CTM model is much easier than microscopic models to calibrate and use to specify strategies to improve freeway operations and to evaluate their potential benefits. The calibrated CTM model for I-880N generates behavior that agrees closely with empirical measurement, including location of bottlenecks, propagation of congestion upstream from bottlenecks, hourly delay and travel time. The validity of the model is further confirmed by comparing its performance under a simulated accident with empirical measurements. This lends confidence to the model's prediction of major reductions in delay by appropriate ramp metering.

ACKNOWLEDGEMENT

This work is supported by the California Department of Transportation through the California PATH Program. The contents of this paper reflect the views of the author and not necessarily the official views or policy of the California Department of Transportation. The results reported here are due to the TOPL Group, especially Gabriel Gomes, Roberto Horowitz, Alex Kurzhanskiy and Jaimyoung Kwon. This paper was written while the author was Visiting Distinguished Professor at the University of Hong Kong. It is a pleasure to acknowledge the hospitality of the Department of Electrical and Electronic Engineering.

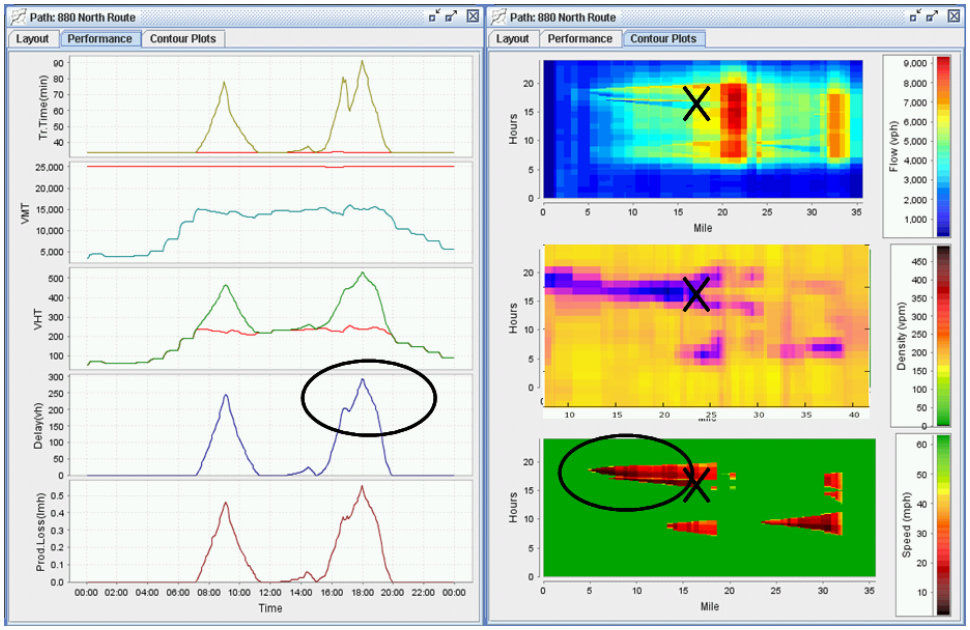

Figure 8: Simulation of an accident that shuts down two lanes from 3:40 until 4:45PM.

References

California Center for Innovative Transportation. Corridor management plan demonstration: Final report. Technical report, University of California, Berkeley, 2006. http://www.calccit.org/resources/2007_PDF/CCIT_TO3_FinalReport-Jan5-07.pdf.

California Department of Transportation. Strategic Growth Plan, 2006. www.dot.ca.gov/docs/strategicgrowth.pdf-2006-10-10.

G. Gomes, R. Horowitz, A.A. Kurzhanskiy, P. Varaiya, and J. Kwon. Qualitative theory of the cell transmission model. *Transportation Research Part C*, 2007. In press: doi:10.1016/j.trc.2007.10.005.

M. Papageorgiou, H. Hadj-Salem, and J. Blosseville. ALINEA: a local feedback control law for on-ramp metering. *Transportation Research Record*, 1320:58–64, 1991.

M. Papageorgiou, H. Hadj-Salem, and F. Middleham. ALINEA local ramp metering: Summary of field results. *Transportation Research Record*, 1603:90–98, 1997.

PeMS. PeMS website, 2007. http://pems.eecs.berkeley.edu, accessed 8/28/2007.

X. Sun and R. Horowitz. Set of new traffic-responsive ramp-metering algorithms and microscopic simulation results. *Transportation Research Record*, 1959:9–18, 2006.

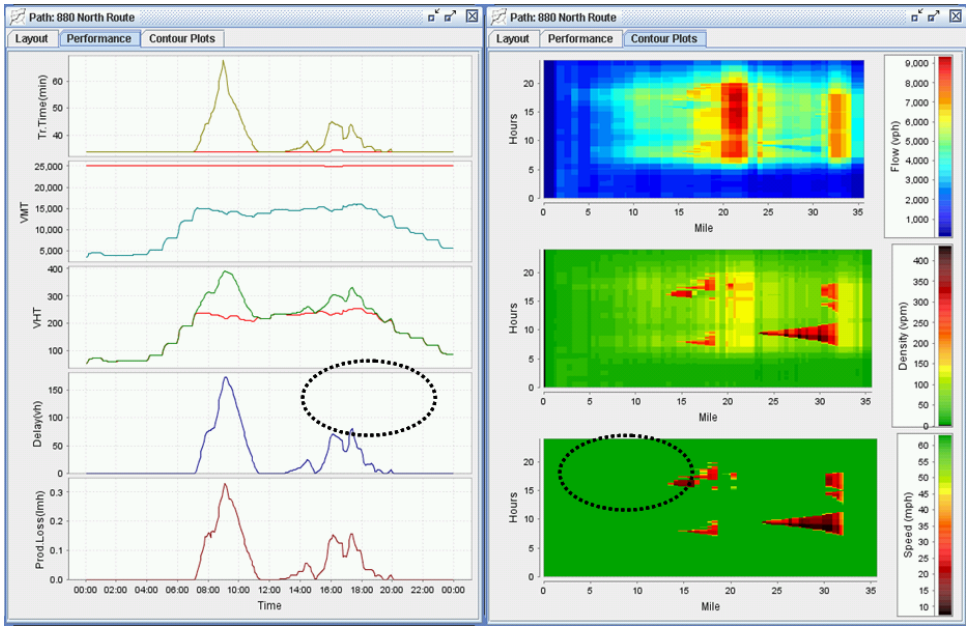

Figure 9: Simulation of the accident with ramp metering in place.

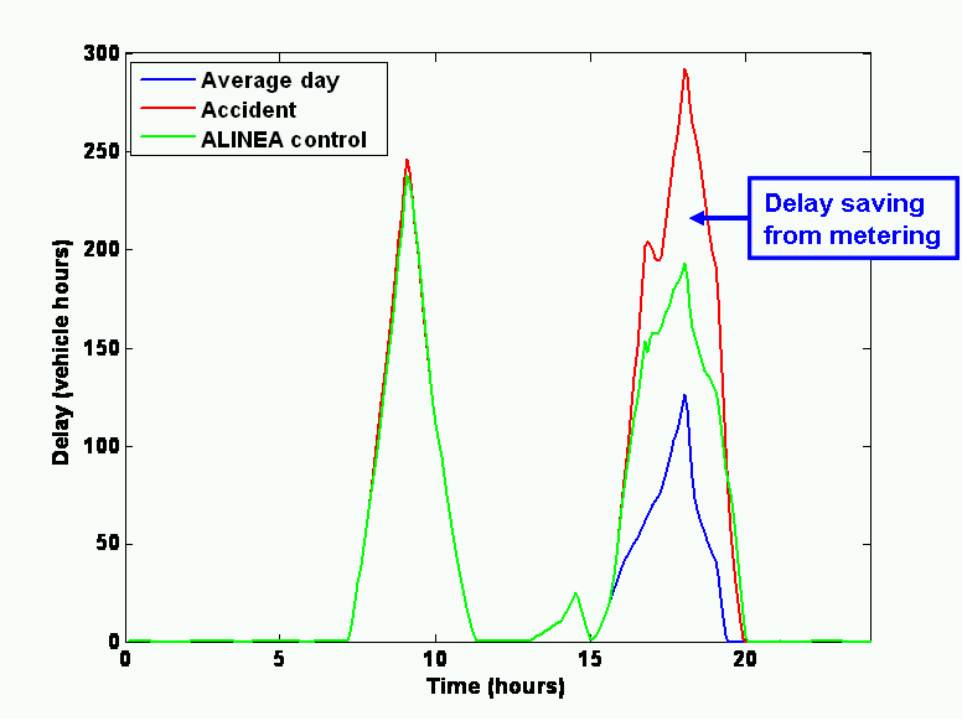

Figure 10: Plots of hourly delay: base case (bottom), with accident (top) and under metering (middle) .

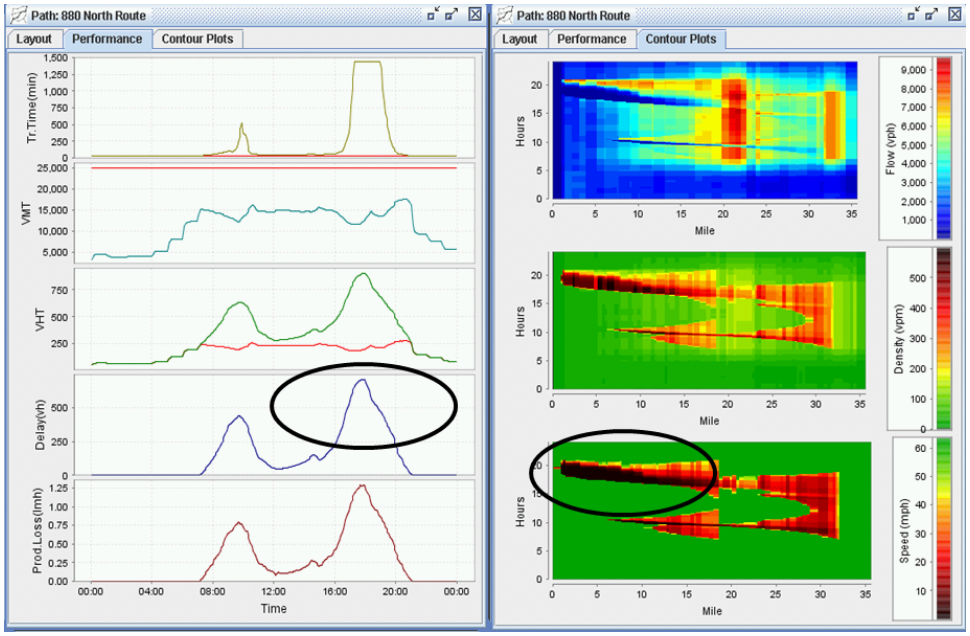

Figure 11: Simulation of a two percent increase in demand.

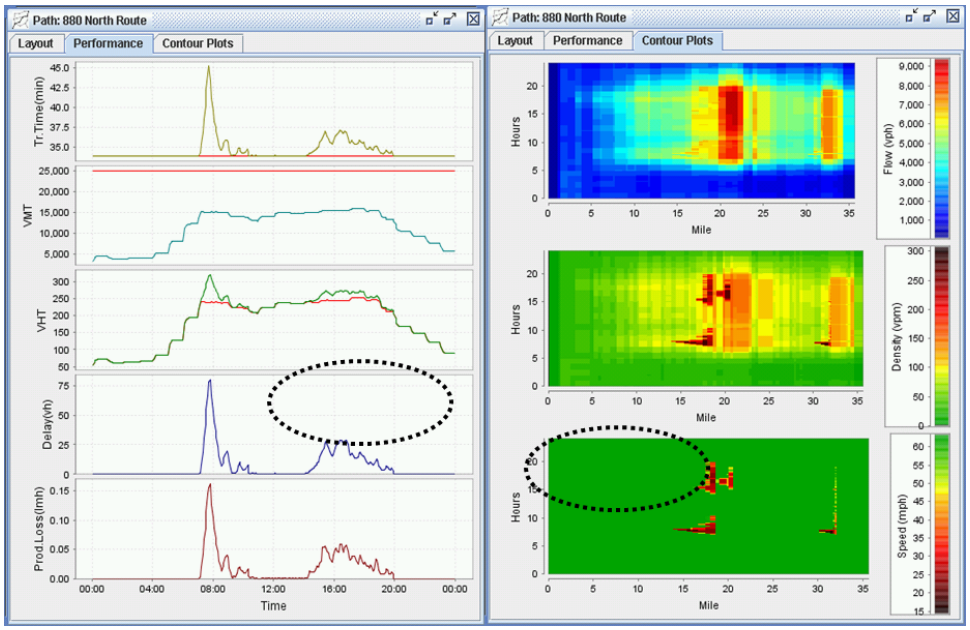

Figure 12: Simulation of the increased demand under metering.

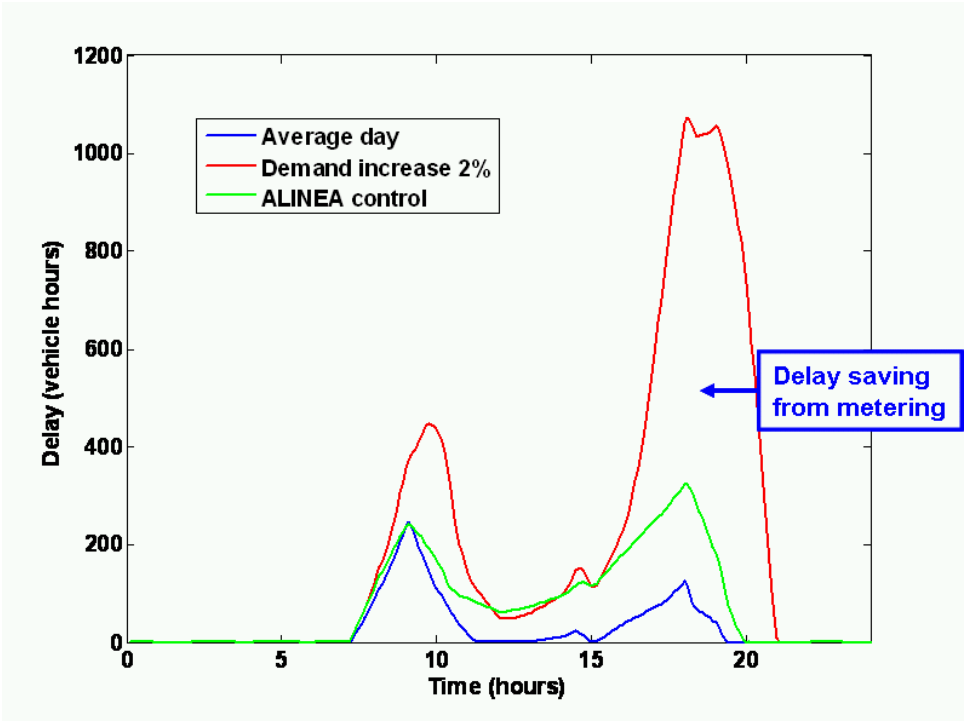

Figure 13: Plots of hourly delay: base case (bottom), with accident (top) and under metering (middle) .